



Twisted laminar superconducting composite: MgB_2 embedded carbon nanotube yarns

U LAMICHHANE¹, G C DANNANGODA¹, M A HOBOSYAN¹, R A SHOHAN¹,
A ZAKHIDOV^{2,3,4} and K S MARTIROSYAN^{1,*} 

¹Department of Physics and Astronomy, University of Texas Rio Grande Valley, Brownsville, TX 78520, USA

²NanoTech Institute, University of Texas at Dallas, Richardson, TX 75083, USA

³Department of Physics and Engineering, ITMO University, Lomonosov str. 9, Saint Petersburg, Russia 191002

⁴National University of Science and Technology, NUST-MISIS, Leninsky pr. 4, Moscow, Russia 119049

*Author for correspondence (karen.martirosyan@utrgv.edu)

MS received 9 June 2021; accepted 7 August 2021

Abstract. Twisted laminar superconducting composite structures based on multi-wall carbon nanotube (MWCNT) yarns were crafted by integrating magnesium and boron homogeneous mixture into the carbon nanotube (CNT) aerogel sheets. After the ignition of the Mg–B–MWCNT system, under the controlled argon environment, the high exothermic reaction between magnesium (Mg) and boron (B) with stoichiometric ratio produced the MgB_2 @MWCNT superconducting composite yarns. The process was conducted under the controlled argon environment and uniform heating rate in the differential scanning calorimetry and thermogravimetric analyzer. The XRD analysis confirmed that the produced composite yarns contain nano and microscale inclusions of superconducting phase of MgB_2 . The mechanical properties of the composite twisted and coiled yarns at room temperature were characterized. The tensile strength up to 200 MPa and Young's modulus of 1.27 GPa proved that MgB_2 @MWCNT composite is much stiffer than single component MgB_2 wires. The superconductive critical temperature of $T_c \sim 38$ K was determined by measuring temperature-dependent magnetization curves. The critical current density, J_c of superconducting component of composite yarns was obtained at different temperatures below T_c by using magnetic hysteresis measurement. The highest value of $J_c = 3.39 \times 10^7$ A cm⁻² was recorded at 5 K.

Keywords. Magnesium diboride; twisted laminar composite; superconducting material; multi-wall carbon nanotube; magnetic hysteresis.

1. Introduction

The discovery of superconductivity in a simple hexagonal binary compound of MgB_2 as a type II superconductor renewed the interest in the field of superconductivity at a relatively high critical temperature of ~ 39 K [1]. The widespread applications of MgB_2 lead to the manufacture of commercial superconducting wires. Superconducting technology has made significant progress for the development of magnetic shielding systems to protect space station crews from the ionizing radiation encountered during long-term missions [2,3]. Multiple research groups work for the enhancement of critical current density, J_c by the introduction of flux pinning centres [4–7]. With its large coherence length and double gap superconductivity, various practices including doping with a variety of additives, thermo-mechanical processing and magnetic shielding have been introduced in the last decades. The deposition of FeO nanoparticles on the surface of MgB_2 thin films [4], Ti doping with MgB_2 [5], multiwall carbon nanotube

(MWCNT) doping on MgB_2 /Fe monofilament wires [6], MgB_2 @MWCNT composite wire fabrication [7] are some practices of impurity scattering by introducing some defects into the two-band MgB_2 . Magnesium diboride MgB_2 has been successfully synthesized under argon in ambient, elevated and high pressures by using high exothermic self-propagation reaction between initial components [8,9]. Higher J_c in a superconducting material is an essential aspect for efficient transmission of energy, and it is vital for saving energy and future power applications of MgB_2 superconducting wires.

The improvement in J_c can be achieved by the partial substitution of a small amount of dopant, such as SnO_2 [10], Zr precursors [11,12], Dy_2O_3 [13], Pr_6O_{11} [14] and C precursors, which can increase the scattering by impurity due to the chemical disorder. Introducing more pinning centres, especially nano-sized second phase inclusions, provided a strong pinning force. Eventually, increasing the number of pinning centres close to the grain boundaries can significantly increase the J_c value. Among the various dopants, the

dopants of C precursors including carbon nanotubes (CNTs) is more effective compared to other sources because of their high aspect ratio and nanometre size [15–19]. Furthermore, the interior thermal stability, heat dissipation and mechanical strength of MgB_2 superconducting wire can be improved by the influence of CNTs. MWCNTs can carry current densities up to $10^9\text{--}10^{11} \text{ A cm}^{-2}$ [20] and may have a thermal conductivity of $3000 \text{ W m}^{-1} \text{ K}^{-1}$ [21]. In addition, they can improve the current path and connectivity between the grains in MgB_2 .

In this study, we show proof-of-concept of a synthetic route for the effective preparation of twisted laminar MgB_2 @MWCNT composite superconducting yarns by uniformly heating the homogenous mixture of Mg–B powders embedded inside the twisted MWCNT yarn. Since MWCNTs are very stable at the high temperature and its melting point is above 3000°C , we used MWCNT as a matrix host structure to arrange the laminar superconductive flexible wire by initiating a combustion reaction: $\text{Mg} + 2\text{B} \rightarrow \text{MgB}_2$ inside the MWCNT yarn. Moreover, the elemental form of Mg and B powders heated inside the MWCNT laminar matrix structure helps to increase the number of pinning centres inside the grains of MgB_2 phase, which assists in the improvement of J_c . Somehow, similar composites of MgB_2 coated on MWCNT fibres have been created earlier by quite complicated method of B laser deposition followed by exposure to mg vapours in vacuum [25]. We demonstrate here, a much more simple and reliable method, which is a direct combustion reaction within a porous host, after the twist yarn is created with a non-reacted powder of elemental Mg and B. A motivation for using MWCNT laminar structure as a host for superconducting MgB_2 is to provide a strong and stable conductive framework as well as providing carbon doping of MgB_2 by creating scattering centres to improve the superconducting properties of the flexible MgB_2 @MWCNT composites. Moreover, twisted laminar composites superconducting yarns have demonstrated elevated mechanical properties and can be potentially used as an active element to create magnetic field to shield spacecraft from high-energy particles for space application.

2. Experimental methods and procedure

Mixture of magnesium (Mg) and boron (B) powders was prepared by mixing Mg (99%) with a particle size of $\sim 60 \mu\text{m}$ (Sigma Aldrich Co.) and B with a particle size of $\sim 1 \mu\text{m}$ ($\geq 95\%$ amorphous, Sigma Aldrich Co.) according to the stoichiometric ratio of 1:2. Isopropyl alcohol (anhydrous, 99.5%) was introduced to prepare the mixture for milling process. The powder mixture was milled for 3 h using a rotatory ball miller to obtain homogeneous powder mixture. The milling media consists of stainless steel jar with zirconia balls of 5 mm in diameter. The mixture was

then heated in an oven at 60° for 12 h to evaporate isopropyl alcohol.

MWCNTs were extracted from CVD grown vertically aligned (VA) CNTs forest (VA-CNT). The synthesized forest had a CNT with an average diameter of $\sim 10 \text{ nm}$. The $280 \mu\text{m}$ tall forest had a volumetric forest density of 63.8 mg cm^{-3} . It is well known that CNT can carry very high current densities due to their very high thermal stability and low temperature coefficient of resistivity [20], although their conductivity is not higher than that of the best metals. It has been shown that till 250°C , no measurable changes in resistivity of MWCNT can be observed at J of 10^9 A cm^{-2} [20].

MWCNT sheets of 1.2 cm wide and 7 cm long were dry drawn from vertically aligned MWCNT forest grown by advanced chemical vapour deposition (CVD) process [22–25] on Fe nanocatalyst-coated Si substrates. The 30 uniform sheets were stacked on the top of each other to increase its strength. The homogeneous mixture of Mg and B was uniformly deposited over the free standing MWCNT sheets: i.e., the MWCNT sheets were coated with magnesium and boron particles by using automated dispensing robot EFD-325TT equipped with a Paasche VL-SET air-brush system. The coating solution was prepared by suspending 25 mg ml^{-1} of Mg–B powder mixture in isopropanol and sonicating for 30 min. The robot was programmed to coat the sheets in 30 s time interval to allow the evaporation of isopropanol and control the MgB_2 @-MWCNT weight ratio. The uniformity was determined by visual examination via optical microscope and low-magnification SEM observations. The twisted laminar yarn was developed by rolling the MgB_2 @MWCNT sheets with a low-speed motor under a constant speed of 30 rpm as described in reference [26]. The mass ratio of MWCNTs to reactive powder mixture was 1:3.

Then, the yarn was heated at the constant heating rate of 20 and 50°C per minute up to 800°C using differential scanning calorimeter and thermogravimetric analyzer (DSC–TGA) (STD-Q600, TA Instruments) to initiate reaction within the CNT matrix. Heating was performed under the Argon atmosphere with 100 ml min^{-1} flow speed. The Mg and Mg–B powders were loosely added to the DSC crucible without compaction.

X-ray diffraction (XRD) measurement of the particles was performed using Bruker D2 Phaser 2nd generation diffractometer with $\text{CuK}\alpha$ radiation ($\lambda = 1.54056 \text{ \AA}$) to confirm the presence of MgB_2 phase. The JSM-7100F, thermal field emission scanning electron microscope equipped with an electron dispersive X-ray spectroscopy system was used for the particle topography and size analysis. The magnetization measurements were performed over the temperature range of 5–50 K and the magnetic field up to 2 T with a quantum design physical properties measurement system (PPMS) equipped with vibrating sample magnetization (VSM) attachment. The mechanical properties were characterized by measuring the tensile

strength and Young's modulus at room temperature in universal testing machine (UTM).

3. Results and discussion

Combustion synthesis of MgB_2 integrated in the MWCNT laminate twisted yarns has been accomplished by volume combustion reaction using DSC. Figure 1a shows the results of DSC–TGA measurement of $\text{MgB}_2/\text{MWCNT}$ yarn exhibiting heat flow evolution and change in wt% at the heating rate of $20^\circ\text{C min}^{-1}$. The initial endotherm in the graph indicates that there is a phase transition (melting) of Mg at about 651°C , before exothermic peak. Once the Mg melts, it reacts with the elemental boron, subsequently releasing a large amount of heat. This exothermic reaction is observable by the peak at $\sim 666^\circ\text{C}$ and the amount of heat released was 777 J g^{-1} . During this exothermic process, some parts of Mg escaped the system due to vapourization at high combustion temperature. The blue line in the graph indicates the percentage of weight changes of the sample at various temperatures. Thus, the $\sim 9.2\%$ decrease in wt% after 66°C is due to the loss of some Mg via evaporation.

For comparison, the DSC experiment was conducted with a mixture of Mg and B powders without integration into the

MWCNT yarns. Figure 1b shows the DSC–TGA result of Mg and B powders reaction under argon environment and uniform heating rate of $20^\circ\text{C min}^{-1}$ up to 800°C . The comparison of the graphs in figure 1a and b shows that the phase transition temperature (melting) in the case of $\text{MgB}_2/\text{MWCNT}$ yarn was decreased slightly compared to the pure MgB_2 powder sample. The amount of heat captured inside the laminar matrix structure creates a slight increase in the force pressure inside the twisted yarn and this pressure lowers the melting temperature. However, the temperature difference is not remarkably large enough to influence the combustion reaction. Similarly, the comparison between the heat release in the exothermic reaction indicates that more heat is released in the case of $\text{MgB}_2/\text{MWCNT}$ composite yarn. The greater rate of heat flow indicated that the complete reaction occurred inside the laminar yarns. However, the weight loss graph in both cases are comparable. It shows that in both the cases, the loss of mass was due to evaporation of Mg. The weight loss in the reaction due to the evaporation of Mg is confirmed by comparing it with the graph in figure 1c. It shows the DSC–TGA results for Mg/MWCNT laminar yarn with an identical experiment. In this case, all the experimental procedures were similar as in the case of figure 1a except the powder inside the yarn was only single Mg. If we compare those results with the weight loss graph in

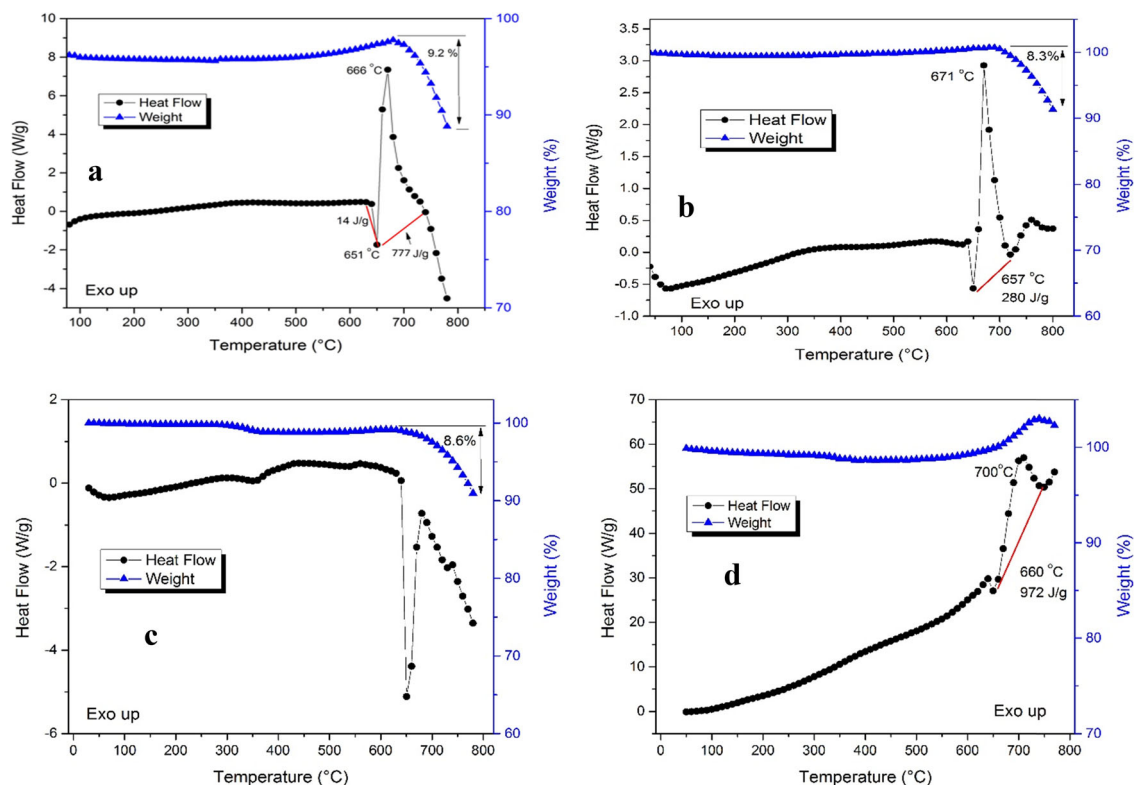


Figure 1. DSC plot showing heat flow and change in wt% at the heating rate of $20^\circ\text{C min}^{-1}$ for (a) $\text{MgB}_2/\text{MWCNT}$ laminar yarn composites; (b) MgB_2 powder sample; and (c) Mg/MWCNT laminar yarn. (d) DSC–TGA results for $\text{MgB}_2/\text{MWCNT}$ yarn under the argon environment at $50^\circ\text{C min}^{-1}$ heating rate.

figure 1a–c, the weight loss is similar in all the cases. This proves that the weight loss is due to the evaporation of Mg powder alone in all the cases. To keep stoichiometric ratio of MgB_2 the amount of Mg was accordingly increased by $\sim 10\%$, while making the powder mixture. At high temperature, some oxidation of MgB_2 results in the increase of mass.

For comparison, identical experiments were performed for different heating rates as well. Figure 1d shows the DSC–TGA results for MgB_2 @MWCNT yarn under the argon environment at accelerated $50^\circ\text{C min}^{-1}$ heating rate. Increasing the heating rate has enhanced the heat of reaction up to 972 J g^{-1} and decreased the Mg mass loss up to 1.32% during the combustion reaction, indicating rapid reaction between reactants and showed that magnesium evaporation was not sufficient at the higher heating rates.

XRD measurement in figure 2 confirms that the yarns are comprised of pure crystalline magnesium diboride (MgB_2) phase within a composite with MWCNT yarns. According to the standard JCPDS card (74-0982), the diffraction data confirms the hexagonal crystal structure of MgB_2 with cell parameters of $a = 3.085$ and $c = 3.523 \text{ \AA}$ and density of 2.6279 g cm^{-3} . The crystallite size calculation has been carried out with the Scherrer's formula [27], $D = \frac{K\lambda}{\beta \cos \theta}$, where K is the constant ($k = 0.94$), λ the wavelength of X-ray, β full-width at half maximum in radians of the selected peak and θ the Bragg's diffraction angle. The calculated crystallite size for (101) peak ($2\theta = 42.43^\circ$) is 21 nm.

Particle morphology was analysed using SEM images as presented in figure 3. The MgB_2 has a laminar structure and the combustion product consists of heterogeneously distributed grains having well-connected particle conglomerates of predominantly particles with average size of about $\sim 1 \mu\text{m}$.

The dimensions of the resulting yarn were $\sim 4 \text{ cm}$ length and 1.4 mm of diameter. The SEM images also confirm the

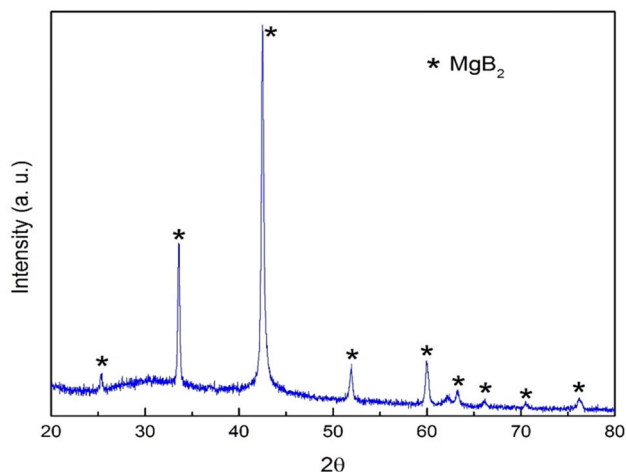


Figure 2. XRD pattern of MgB_2 sample after heat treatment.

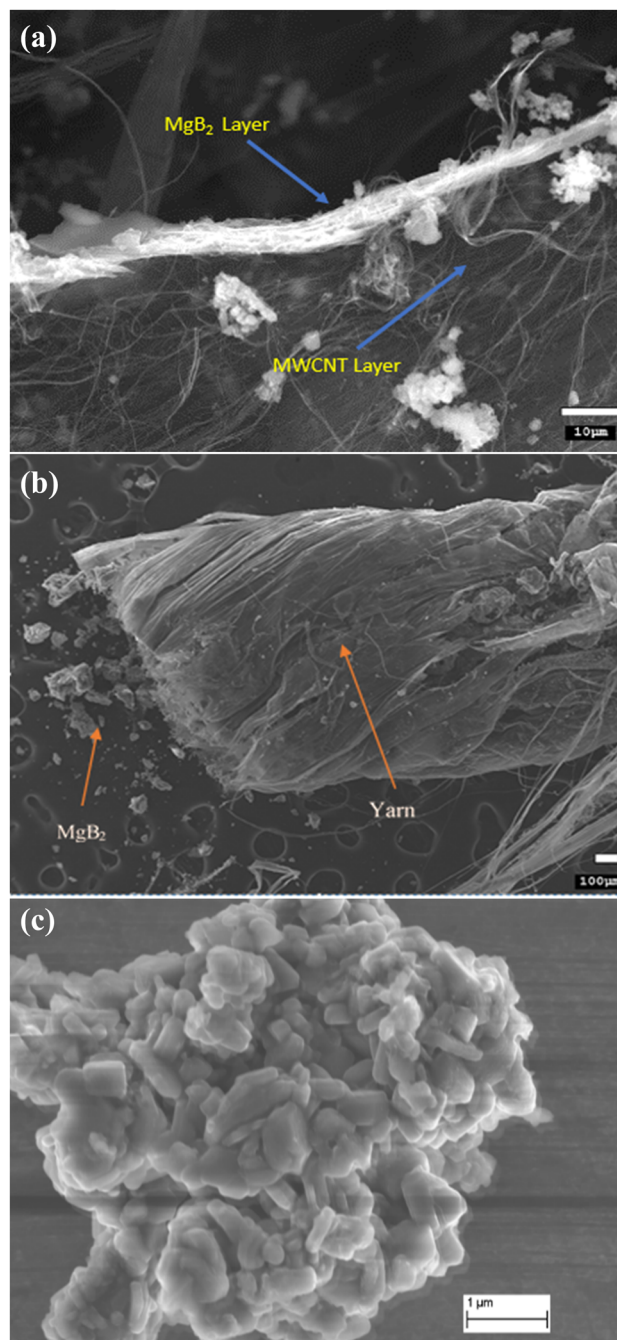


Figure 3. SEM images of (a and b) MgB_2 powder inside the MWCNT yarn; and (c) MgB_2 powder after combustion.

continuous layer of superconducting MgB_2 composites inside the twisted yarn.

The MWCNT twist yarns without Mg/B powder integration have initial tensile stress value of 227 MPa [26]. Figure 4 shows the tensile strength measurement of the MgB_2 @MWCNT yarn at room temperature. The experiments revealed the tensile stress of the integrated yarn composites at maximum load, was about 200 MPa. This value is higher when compared with the transverse compressive stress of 160 MPa for the Fe-sheath PIT processed

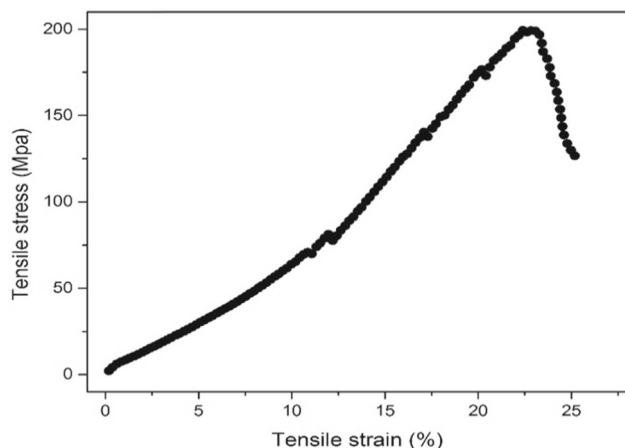


Figure 4. Tensile strength measurement of $\text{MgB}_2/\text{MWCNT}$ yarn.

MgB_2 wire and comparable to internal Mg diffusion (IMD) process MgB_2 wire having 206 MPa compressive stress as reported by Nishijima *et al* [28]. This tensile stress is also higher than the Cu-sheath MgB_2 wire as reported by Kazumune *et al* [29]. The Young's modulus of 1.27 GPa proved that $\text{MgB}_2/\text{MWCNT}$ composite wire is stiffer than single MgB_2 wires. The lower percentage of extension leads to the higher value of Young's modulus.

Temperature dependence of the magnetization curve is shown in figure 5. Zero-field-cooling (ZFC) and field-cooling (FC) magnetization curves were measured in the temperature range of 5–50 K using a magnetic field of 100 Oe. ZFC measurements were performed by cooling down the sample from 300 to 5 K without applying any magnetic field. After reaching 5 K, by applying a small magnetic field of 100 Oe, the sample was heated up to 50 K, above the transition temperature, to obtain the ZFC curve. FC curve was obtained by cooling down the

sample from 50 to 5 K, while the magnetic field is applied. The curves show that the superconducting transition temperature for twisted laminar $\text{MgB}_2/\text{MWCNT}$ yarn is about 38 K (figure 5a), which is close to critical temperature of 39 K for pure MgB_2 powder after combustion (figure 5b). The slight decrease in the critical temperature is due to the carbon doping effect within MgB_2 from the MWCNT yarn. It shows that MWCNT yarn also acts as the carbon doping source for MgB_2 , thus, additionally helping to increase the J_c of the wire via scattering on C-dopants.

Figures 6a and b shows the hysteresis diagrams of twisted laminar $\text{MgB}_2/\text{MWCNT}$ yarn and MgB_2 powder, respectively. For both the cases, the maximum magnetic field of 2 T was applied, and the hysteresis measurement was performed for different temperatures. These typical hysteresis loops display characteristic behaviour of type II superconductor which confirms that produced $\text{MgB}_2/\text{MWCNT}$ samples retain type II superconducting behaviour. The width between highest and lowest magnetization (M) values for a given magnetic field of the hysteresis curve at the point of expulsion of the magnetic field was used to calculate the J_c of the produced superconducting composites. The comparison of figure 6a and b clearly shows that the width of the hysteresis curve increases nearly 10 times in the case of $\text{MgB}_2/\text{MWCNT}$ yarns in comparison to the pure MgB_2 powders. Since the J_c depends on the width of the hysteresis curve and grain size of the sample, it can be inferred from the above diagram that the J_c in the case of $\text{MgB}_2/\text{MWCNT}$ is much higher than the pure MgB_2 . It is apparent from the graphs that as a typical superconductive behaviour, the width of the hysteresis loop decreases, while the temperature increases for both the cases. The width, 67 emu g^{-1} , recorded for 5 K temperature was the highest obtained and it gradually decreased to the lowest value of 25 emu g^{-1} , when the temperature was at 25 K. This also infers that the behaviour of the J_c of a typical

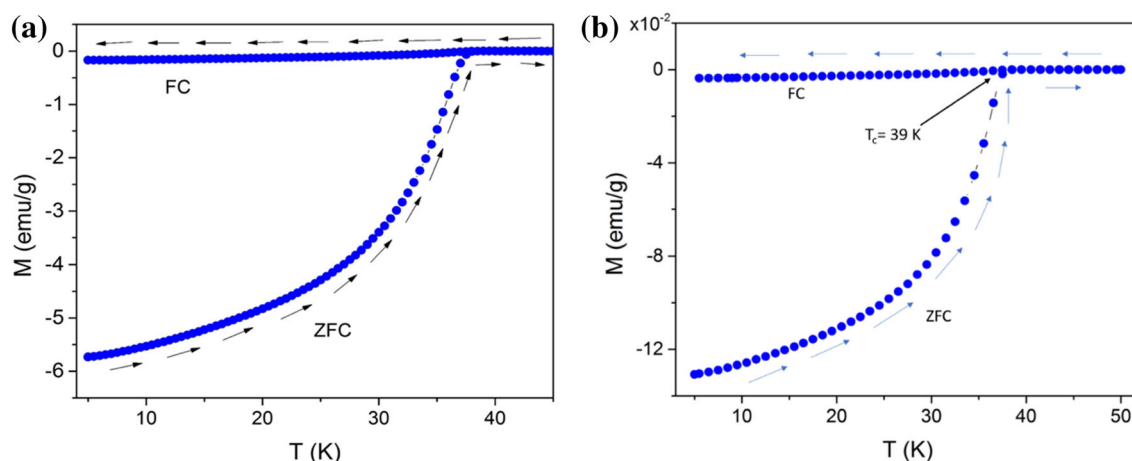


Figure 5. Temperature dependence magnetization curves of (a) twisted laminar superconducting composite $\text{MgB}_2/\text{MWCNT}$; and (b) MgB_2 powder after combustion.

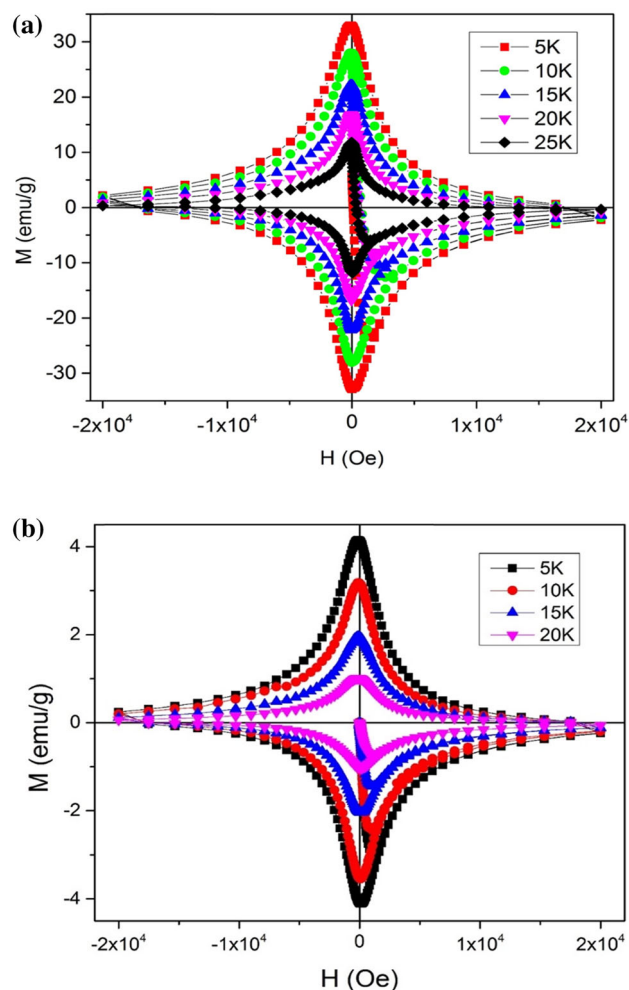


Figure 6. Hysteresis curve of (a) twisted laminar MgB₂/MWCNT yarn and (b) MgB₂ powder samples up to 20 kOe (2 Tesla) at different temperatures.

superconductor, where J_c increases, while the temperature decreases much below T_c . The J_c of the yarn is calculated by using Bean's model [30].

$$J_c = 20 \frac{\Delta M}{d},$$

$$\Delta M = M^+ + M^-,$$

where ΔM is the hysteresis of the magnetization per unit volume (emu cm^{-3}) and d the mean size of particles. The average particle size of 1 μm for MgB₂@MWCNT composite yarn, as confirmed by SEM analysis, was used in the calculation. It shows the magnetization width of hysteresis curves increases as the temperature decreases and hence, the J_c at 5 K is higher as compared to the J_c at 25 K. Figure 7 shows the estimation of J_c values of MgB₂@MWCNT yarn using Bean's formula. The J_c vs. temperature graph indicates that the J_c increases with lowering the temperature. The maximum J_c value obtained at 5 K was $3.39 \times 10^7 \text{ A cm}^{-2}$. Similarly, the J_c values for 10, 15 and 20 K were calculated

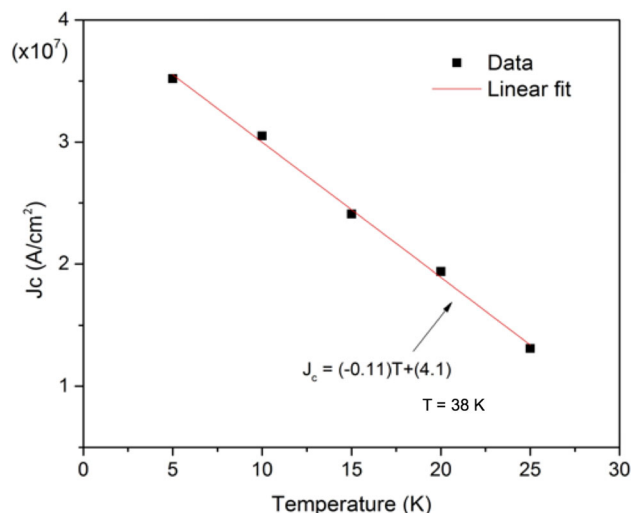


Figure 7. Dependence of critical current density on temperature for MgB₂@MWCNT yarn.

to be 2.88×10^7 , 2.36×10^7 and $1.85 \times 10^7 \text{ A cm}^{-2}$, respectively. The minimum J_c value was estimated at 25 K and it was $1.37 \times 10^7 \text{ A cm}^{-2}$. It should be noted that obtained J_c values for MgB₂@MWCNT twist yarns were well compared in comparison with the J_c values obtained by using MgB₂C₂ with pure C as the carbon source dopant to prepare carbon-doped MgB₂ bulk by *in situ* process with powders in closed-tube method [19], as well as compared to doping/mixing of CNTs in different concentrations in MgB₂ [18]. The enhancement of J_c in MgB₂@MWCNT composites may be attributed to the flux pinning capability of MWCNT in MgB₂ matrix and better grain connectivity [31,32]. There is a strong experimental evidence of improvement in the flux pinning behaviour through varieties of procedures including high energy ion-irradiation [33], chemical doping by metallic and non-metallic phases or nano particles [5,34,35]. A number of experimental data also revealed that chemical doping sufficient approach for increasing J_c of magnesium diboride superconductors [36–40]. It was shown that in the carbon-doped magnesium diboride, the carbon atoms substitute boron sites which strengthen the optical phonon mode and inter-band scattering between the σ - and π -bands [41–45]. Carbon substitution is one of the most effective methods to improve the low-upper critical field and irreversibility field because of the increased scattering by C doping. The atomic replacement shifts the Fermi level and enhances impurity scattering, thus increasing the upper critical field and introduces point defects which act as the pinning centres leading to the higher irreversibility field and J_c .

The MgB₂@MWCNT composites, when properly optimized for better interconnectivity of MgB₂ grains (as demonstrated in reference [25]), can be potentially used for fabricating superconducting magnet systems that can generate strong fields, e.g., to shield spacecrafts from cosmic radiation for the long periods of time, since MWCNTs have enhanced radiation stability.

4. Conclusions

MgB₂ embedded into MWCNT superconducting twisted laminar yarns can be fabricated by an exothermic interaction of Mg and B powders inside the MWCNT yarn matrix via the combustion reaction under argon environment. The twisted yarn shows the superconducting transition at 38 K. The use of MWCNT yarn increases the tensile strength and Young's modulus of superconducting MgB₂/CNT composites as compared to the superconducting MgB₂ wires developed via conventional PIT method. The increase in J_c proves that MgB₂@MWCNT composite yarns have more effective approach than just random CNT doping into bulk MgB₂. The maximum value of $J_c = 3.39 \times 10^7$ A cm⁻² was obtained for MgB₂ embedded MWCNT twisted yarns. The improved J_c and the strong mechanical and physical properties of MWCNT can be combined in the form of superconducting twisted composite yarns to produce low-cost high-performance commercial superconducting composite yarns wires for various high-power applications. Scaling up of the fabrication of superconducting twisted laminar yarns is possible using furnaces with controlled inert atmosphere and associated heating rate replicating the DSC conditions.

Acknowledgements

We would like to acknowledge the partial financial support for this research by National Science Foundation awards 1126410 and DMR-1523577, Welch Foundation grant AT 1617, the Ministry of Education and Science of the Russian Federation (Project 14.Y26.31.0010), Russian Science Foundation (no. 19-73-30023) and partially by Increase Competitiveness Program of NUST "MISiS" (no. K2-2015–014).

References

- [1] Jun N, Nakagawa N, Muranaka T, Zenitani Yu and Akimitsu J 2001 *Nature* **410** 63
- [2] Musenich R, Calvelli V, Farinon S, Battiston R, Burger W J and Spillantini P 2014 *IEEE Trans. Appl. Supercond.* **24** 4601504
- [3] Musenich R, Nardelli D, Brisigotti S, Pietranera D, Tropeano M, Tumino A *et al* 2015 *IEEE Trans. Appl. Supercond.* **26** 6200204
- [4] Surdu A E, Hamdeh H H, Al-Omari I A, Sellmyer D J, Socrovisciuc A V, Prepelita A A *et al* 2011 *Beilstein J. Nanotechnol.* **2** 809
- [5] Zhao Y, Feng Y, Cheng C H, Zhou L, Wu Y, Machi T *et al* 2001 *Appl. Phys. Lett.* **79** 1154
- [6] Kim J H, Yeoh W K, Qin M J, Xu X and Dou S X 2006 *J. Appl. Phys.* **100** 013908
- [7] Dipak P, Maeda M, Choi S, Kim S J, Shahabuddin M, Parakandy J M *et al* 2014 *Scr. Mater.* **88** 13
- [8] Tolendiyuly S, Fomenko S M, Abdulkarimova R G, Mansurov Z A, Dannangoda G C and Martirosyan K S 2016 *Int. J. Self-Propagat. High-Temp. Synth.* **25** 97
- [9] Tolendiyuly S, Fomenko S M, Dannangoda G C and Martirosyan K S 2017 *Eurasian Chemico-Technol. J.* **19** 177
- [10] Zhang D, Sumption M D, Collings E W, Thong C J and Rindfleisch M A 2019 *IEEE Trans. Appl. Supercond.* **29** 1
- [11] Feng Y, Zhao Y, Sun Y P, Liu F C, Fu B Q, Zhou L *et al* 2001 *Appl. Phys. Lett.* **79** 3983
- [12] Yanwei M, Kumakura H, Matsumoto A, Hatakeyama H and Togano K 2003 *Supercond. Sci. Technol.* **16** 852
- [13] Chen S K, Wei M and MacManus-Driscoll J L 2006 *Appl. Phys. Lett.* **88** 192512
- [14] Pan X F, Shen T M, Li G, Cheng C H and Zhao Y 2007 *Phys. Status Solidi* **204** 1555
- [15] Kim J H, Yeoh W K, Xu X, Dou S X, Munroe P, Rindfleisch M *et al* 2006 *Phys. C: Supercond. Appl.* **449** 133
- [16] Dou S X, Yeoh W K, Horvat J and Ionescu M 2003 *Appl. Phys. Lett.* **83** 4996
- [17] Kim J H, Yeoh W K, Qin M J, Xu X, Dou S X, Munroe P, Kumakura H *et al* 2006 *Appl. Phys. Lett.* **89** 122510
- [18] Chandra S, Giri R, Malik S K and Srivastava O N 2007 *J. Nanosci. Nanotechnol.* **7** 1804
- [19] Momoko S, Shimoyama J, Takagi N, Motoki T, Kodama M and Tanaka H 2018 *Solid State Commun.* **281** 53
- [20] Wei B Q, Vajtai R and Ajayan P M 2001 *Appl. Phys. Lett.* **79** 1172
- [21] Kim P, Li S, Arun M and McEuen P L 2001 *Phys. Rev. Lett.* **87** 215502
- [22] Baughman R H, Zakhidov A A and De Heer W A 2002 *Science* **297** 787
- [23] Zhang M, Atkinson K R and Baughman R H 2004 *Science* **306** 1358
- [24] Zakhidov A A, Baughman R H, Iqbal Z, Cui Ch, Khayrullin I, Dantas S O *et al* 1998 *Science* **282** 897
- [25] Bykova J S, Lima M D, Haines C S, Tolly D, Salamon M B, Baughman R H *et al* 2014 *Adv. Mater.* **26** 7510
- [26] Hobosyan M A, Martinez P M, Zakhidov A A, Haines C S, Baughman R H and Martirosyan K S 2017 *Appl. Phys. Lett.* **110** 203101
- [27] Langford J I and Wilson A J C 1978 *J. Appl. Crystallogr.* **11** 102
- [28] Nishijima G, Ye S J, Matsumoto A, Togano K, Kumakura H, Kitaguchi H *et al* 2012 *Supercond. Sci. Technol.* **25** 054012
- [29] Kazumune K, Takaya R, Kasaba K, Tachikawa K, Yamada Y, Shimura S *et al* 2005 *Supercond. Sci. Technol.* **18** S351
- [30] Bean C P 1964 *Rev. Mod. Phys.* **36** 31
- [31] Shekhar Ch, Giri R, Tiwari R S and Srivastava O N 2007 *J. Appl. Phys.* **102** 093910
- [32] Yeoh W K, Kim J H, Horva J, Dou S X and Munroe P 2006 *Supercond. Sci. Technol.* **19** 2
- [33] Pallecchi I, Tarantini C, Aebbersold H U, Braccini V, Fanciulli C, Ferdeghini C *et al* 2005 *Phys. Rev. B* **71** 212507
- [34] Choi E M, Lee H S, Kim H, Lee S I, Kim H J and Kang W N 2004 *Appl. Phys. Lett.* **84** 82
- [35] Wang S F, Dai S Y, Zhou Y L, Zhu Y B, Chen Z H, Lü H B and Yang G Z 2004 *J. Supercond.* **17** 397
- [36] Shekhar C, Giri R, Tiwari R S, Rana D S, Malik S K and Srivastava O N 2005 *Supercond. Sci. Technol.* **18** 1210
- [37] Wang J, Bugoslavsky Y, Berenov A, Cowey L, Caplin A D, Cohen L F *et al* 2002 *Appl. Phys. Lett.* **81** 2026
- [38] Shen T M, Li G, Zhu X T, Cheng C H and Zhao Y 2005 *Supercond. Sci. Technol.* **18** L49

- [39] Bhatia M, Sumption M D, Collings E W and Dregia S 2005 *Appl. Phys. Lett.* **87** 042505
- [40] Kim J H, Dou S X, Oh S, Jercinovic M, Babic E, Nakane T and Kumakura H 2008 *J. Appl. Phys.* **104** 063911
- [41] Wilke R H T, Bud'ko S L, Canfield P C, Finnemore D K, Suplinskas R J and Hannahs S T 2004 *Phys. Rev. Lett.* **92** 217003
- [42] Kazakov S M, Puzniak R, Rogacki K, Mironov A V, Zhigadlo N D, Jun J *et al* 2005 *Phys. Rev. B* **71** 024533
- [43] Eisterer M 2007 *Supercond. Sci. Technol.* **20** R47
- [44] Xi X X 2008 *Rep. Prog. Phys.* **71** 116501
- [45] Kim J H, Oh S, Heo Y-U, Hata S, Kumakura H, Matsumoto A *et al* 2012 *NPG Asia Mater.* **4** e3